Determination of Critical Overload Transmission Line Using Novel Maximum Power Line Stability Index

A. A. Emhemed[1], R. Ishat[2], A.N. Abdalla[3]

[1,2]Department of Electrical and Electronic Engineering, University Malaysia Pahang.
[3]Professor Dr, Faculty of electronic and information engineering, huaiyin institute of technology, Jiangsu, China
Corresponding author E-mail: Missing

Abstract

Recent years, a larger number of DG's are being employed especially at the critical load ends to reduce the burden on the main feeder. One of the benefits of employing DG that it improves the system voltage stability even with load increment. The primary focus of this paper rests on creating a novel line voltage stability index. The line stability index approach is proposed based on Thevenin theory to gauge the DG level impact on transmission line. Transmission issues due to the overloading of lines in high DG penetration areas during the outage scenarios taking place earlier. The rationale for the proposed strategy will be experimented on a standard IEEE 30 bus test system compared with other line voltage stability indexes.

Keywords: *Transmission Line; Stability Index; Distributed Generator.*

1. Introduction

Increase in power consumption can cause serious problems in electric power systems if there are no on-going construction projects of new power plants or transmission lines. Additionally, such increase can result in voltage regulation, current and large power losses in the system (1, 2). Experts worldwide have regarded the system protection as the major threat to transmission networks. To date, with the reduced investment of power system expansion, load growth particularly in areas with weak transmission and generation that cause unusual load patterns, the protection system assessment has become of utmost importance and therefore, efforts have been made to develop the theories to facilitate the explanation and analysis (3, 4).

Transmission issues are mainly linked with the overloading of the transmission lines, when all the DG generated cannot be delivered as a whole due to the outage conditions noted previously. In general, DG resources are located at a remote location and this means that they are far from main load centers (5-11). The areas will have restricted transmission capabilities, as they were designed mainly to serve small loads in the area. Under such a scenario, one of the protection issues from a system's point of view lies in the overloading of the transmission lines. The current planning criterion is to weigh upon the DG with high capacity and to curb the capacity or to put in other words, upgrade the constrained transmission interface throughout the system impact study taking into account the N−1 contingencies (10, 12). The system impact study also necessitates the assessment of double (scheduled and/or forced) contingencies close to the proposed generators to determine any operating restrictions under the outage conditions.

Many researches all over the world have labelled system protection as the main threat imposed to transmission networks. In recent times, transmission issues are mainly linked with the issue of the overloading of the transmission lines, when all the wind power generated cannot be fully delivered due to the outage conditions noted earlier. In general, high wind resources are located at a secluded location and are far from the main load centres (13, 14). Different control techniques have been adopted to improve the wind power generation in wind areas that have limited transmission capability. Such a scheme can be applied only for the case where wind farms are located at the tip of interconnection and it is definite that all the power from wind farm is going to flow only via the interconnected transmission line identified. The areas will have scarce transmission capabilities, as the primary aim is to serve small loads in the area. The intense penetration of wind power has turned those areas into large generation areas. Administering such large generations in a weak network with changing generation patterns has contributed to a real operational issue, especially in prior outage scenarios. The cost of spilling of wind energy is weighed against the cost of grid reinforcement that is integrated in the system economically. This brings us to the development of distributed generator (DG) with fault ride through capability either via the control modification and full converter design or through external dynamic reactive support for the squirrel cage machines (6-10) As it is, we cannot run from the limitations in traditional security assessment tools and methods to cater for such characteristics which are specific to wind power.

Distribution systems are operating mostly without installed generation units and radial in nature. The amount and location of power supplied from DG units into the distribution network can determine its operation and they can either lower or add to the system's stability and efficiency. Huge power provided from the DG units can reverse the direction of the power flow. As an instance, the non-optimal location of the DG may induce excess amount of power in the system and this can explain the undesired voltage profiles and an increase in power losses. Therefore, suitable rating and position of the DG units are very critical in ascertaining the system performance (15, 16).

That said, the use of distributed generators has changed the characteristics of network. The conventional distribution system has been designed for a unidirectional power flow; however with the existence of DG; the possibility is that the power flows in both directions. Despites being advantageous, DG could potentially create problem as it alters the technical characteristics of the networks and brings system operation closer to the security limits (17-19). Thus, advanced analysis tools and techniques must be adopted to study the impact of DG accurately.

The main motivation for our current work is derived transmission line stability index through the interaction with the utility. To address the issue of transmission lines overloading in distrusted generator for regulating the generation, increase load and line contingency to check the Maximum line stability index (MLSI) reliability for efficient manner compared with other index. Then, (MLSI) and the continuation power flow are combined to determine the most sensitive load buses to voltage collapse. Lastly, a simulation is conducted on the IEEE 30-bus distribution network with MATLAB to validate the effectiveness of the proposed method. The simulation results indicate that the technique is feasible for practical implementation.

2. Background

There has been an increase in the installation of DG units; therefore, it is very important to look into the impacts towards power system when it comes to the stability, security and reliability. These system parameters are very much affected by DG's size and location hence it is vital to properly select optimal the DG location and size. (10), suggest that the allocation of DG at unsuitable location and beyond particular capacity can have a reverse impact on losses. In several other cases, DGs are located within or close to substation because of accessibility.

2.1 Distributed Generation and Its Impact

Recently, the power industry sector have experience some remarkable changes on its electrical power system due to the incremental implementation of the distributed generation (DG). Although the DG technology was introduced decades ago, it is gaining popularity due to higher demands, more modern technology, better network reliability, economics and environmental concerns. There is a sum of DG technology prevalent in the market today. Distributed generators can use either the renewable or non-renewable energy resources (20-22). The non-renewable DG technologies can be the diesel engine, micro-turbines and fuel cells; while renewable DG technologies include photovoltaic, wind turbines and biomass. DG with renewable technology offers a great opportunity for human exploitation, however often the abundant renewable resources only exist at inaccessible locations thus limits its feasibility as opposed to the non-renewable based DG.

The modern power system is challenged with increasing load demands from the industrial, commercial and residential sectors. The diversity of the load on a system increases as the number of new users increased. Uncertainty and variations in the load demand from different sectors pose additional challenges to be faced by power systems. For heavily loaded system, voltage instability may occur due to lack of power reserves, subsequently, causes the system to lose to maintain the required voltage level. (23).

At present, the number of disruptions occurring in the power industry sector has increase, possibly due to congestions in transmission and distribution systems. The continuous increase in load demand causes the power system to work closely to the system's critical point (24, 25).. To ensure that consumers get constant supplies, some preventive measures have been in the agenda, like improvements in the controlling mechanisms and technology, regular equipment inspection, proper system maintenance and execution of penalties. Nevertheless, it is still common for the disturbances to occur occasionally in the system especially during

peak hours when the power demand is very high. Thus, many organizations need to think for the long sustainable solution with sound flexibility and practicability features. One of the strategies recommended is to generate electricity near to the users' zones. This concept has exuded some appeal in the use of distributed generation technologies as the main choice in the production of electricity in future. Additionally, because of the congestion in the transmission system, the number of occurring disruptions also shows an increase; under these ailing circumstances the scenario might get even graver and further affect the network stability and security. The installation of distributed generation will offer support to the electrical system before, during and after disruptions. Many studies and investigations have illustrated that distributed generation enhances the stability of electric power systems (26-28). Other alternatives like the capacitor placement and feeder reconfiguration can also be instrumental in optimizing the power system, but DG has the tendency to be more economical and it gives additional benefits when compared to some of these alternatives (29).

2.2 Power System Voltage Stability

A power system enters a state of voltage instability when a disturbance results in a progressive and uncontrollable voltage decline. Often the primary causes of this problem are sudden load increase, outages of major generator, outages of transmission line, or a combination of multiple events. The voltage instability incidents have increased widespread with serious power interruptions causing substantial amount of losses and disgrace society approval at large. Voltage stability is defined as the ability of a power system to maintain acceptable voltages at all buses both under normal operating conditions and after being subject to contingency conditions (30-33).

Voltage stability is also the stability of load. Voltage instability is often associated with an increase in load. When there is an increase in the load power demand, the voltage control mechanism in the power system will try to restore the voltage level to normal while meeting the increased load demand. The load restoration continues until further stresses and overloads power system resulting in voltage instability. Voltage collapse often occurs during the final stage of voltage instability when very low bus voltages lead to a partial or total blackout in the system (32).

In electrical, two most common methods been employed for analyzing voltage instability can be distinguished into two categories i.e static and dynamic analysis (24). The objective of the static approach is to determine the system proximity to voltage collapse using either conventional or modified power flow. On the other hand, dynamic analysis is a time domain simulation approach which provides information on mechanisms leading to voltage instability. The dynamic analysis does not provide information regarding the sensitivity or stability margin of a system to collapse point.

Static analysis which also referred to as load-flow or steady-state analysis reveals equilibrium points of a system under study. In static analysis, assessment of power system stability is done using scalar magnitudes, or index. Stability index is a mathematical formulation for estimating the current status of power system and distance to instability, thus development of voltage stability indices is a major concern (34, 35).

On the other hand, the dynamic analysis involves extensive modeling of power system elements through algebra and differential equations approach. The system differential equations are then solved in time domain using various numerical integration methods such as Euler and Range-Kutta methods (31). For a large-scale power system, the dynamic simulation is a time consuming process and relies heavily on computer capacity or performance. Generally, this type of analysis is useful to gain insight into voltage collapse mechanisms and also for coordination of protection and control equipment.

Voltage stability study often requires examination of a wide range of system conditions with various contingency scenarios. Study of stability from static approach becomes attractive as it allows the problems to be examined as a parametric load flow problems that involves much simple computation and shorter time. The method provides a practical and effective solution for many voltage stability problems. A number of static analysis approaches have been initiated by researchers to analyze and to restrict voltage collapse phenomenon for a better power system operation. The various efforts can generally be categorized into a few common schemes such as sensitivity analysis, modal analysis and index based analysis.

voltage stability indices particularly could be subdivided into two parts, which are Jacobian matrix based voltage stability indices and system variables based voltage stability indices. The differences between Jacobian matrix based voltage stability indices and system variables based voltage stability indices is provided in Table 1.

Table 1. Differentiation between Jacobian matrix based voltage stability indices and system variables based voltage stability indices

Jacobian matrix based voltage stability indices	System variables based voltage stability indices
Require more amount of computing time	Require less amount of computing time
Suitable for offline monitoring purpose	Suitable for online monitoring purpose
Discover voltage stability margin	Discover weak buses and lines
(Proximity towards voltage collapse)	(Mechanism of voltage instability)

3. Line Voltage Stability Indices

There are a number of voltage stability indices that can assess the degree of voltage stability and measure the severity of the voltage stability problem. These indices are used to determine the closeness of an operating point to the critical point (36). In voltage stability analysis it is useful to know a given particular operating point of the power system, how far this operating point is to voltage instability. This enables the operators to anticipate and take precautionary measures to avoid any pending voltage instability.

Several voltage stability indices derived from static power flow analysis were proposed for utility power systems. The values of the indices were calculated for each distribution line based on load flow results. The line with the largest value was taken as the weakest line in a system and received special attention to maintain voltage stability. A voltage stability index (LQP) that neglected line resistance was proposed by Kumar & Raju (37).

$$LQP = 4\left(\frac{X}{V_i^2}\right)\left(\frac{X}{V_i^2}P_i^2 + Q_j\right) \leq 1 \tag{1}$$

A fast voltage stability index (FVSI) was derived by Musirin & Rahman (38). The fast index neglected the angle difference between the voltages at both ends of a line. A voltage index was represented by the power injected by the load on a local bus and the power injected from the other buses in a system in Verbic & Gubina (39). The value of FVSI that is evaluated close to 1.00 indicates that the particular line is closed to its instability point which may lead to voltage collapse in the entire system. To maintain a secure condition the value of FVSI should be maintained well less than 1.00.

$$FVSI_{ij} = \frac{4Z^2 Q_j}{V_i^2 X} \tag{2}$$

Moghavvemi & Omar (40) proposed Line Stability Index (Lmn) method for calculating voltage stability factor based on a concept of power flow through a single line. Adopting the technique of reducing a power system network into a single line, the voltage stability factors Lmn is derived and used to examine system stability. If Lmn exceeds the value 1.00, the system will lose its stability under any contingency. In Moghavvemi & Omar (40) an interconnected system is reduced to a single–line network and the applied to assess the overall system stability. Utilizing the same concept but using it for each line of the network, a stability criterion is developed.

$$\frac{4xQ_r}{[V_s \sin(\theta - \delta)]^2} = L_{mn} \leq 1.00 \tag{3}$$

4. The Proposed Index

This section introduce a brief overview of index-based analysis for an assessment of power system condition and also it defines a new line voltage stability index to evaluate the global system voltage stability. The derivation of the proposed index begins by simplifying a large power network and starting on some discussions concerning the principal of voltage stability.

The load-flow analysis involves in calculation power flows through transmission line at specific bus load conditions. Each bus is associated with four quantities: voltage magnitude and angle (V, θ), reactive power Q, and active power P. The node equations used to represent the relationships between network flow currents and bus voltages using the based on Kirchoff Current Law (KCL). The network equations, in terms of network admittance matrix, are given by Equation 4:

$$I = Y_{bus}.V \tag{4}$$

Where
Y_{bus} is the network bus admittance matrix
V is the node voltage vector
For bus k, the node injection current is the sum of all admittances connected to bus k, which is written as:

$$I_k = \sum_{n=1}^{N} Y_{kn} V_n; \quad k, n = 1, 2, \ldots N \tag{5}$$

At bus k, the link between real and reactive power supplied and the current injected into the system at that bus is given as:

$$S_k = V_k I_k^* = P_k + jQ_k \tag{6}$$

And the current is

$$I_k^* = \frac{P_k + jQ_k}{V_k} \tag{7}$$

Where
V is the voltage at specific bus k
Q is reactive power at specific bus k; P is real power at specific bus k
Extending the power Equation (6) to *n-bus* system produces:

$$P_k + jQ_k = V_k \sum_{j=1}^{n} Y_{kj} V_j$$

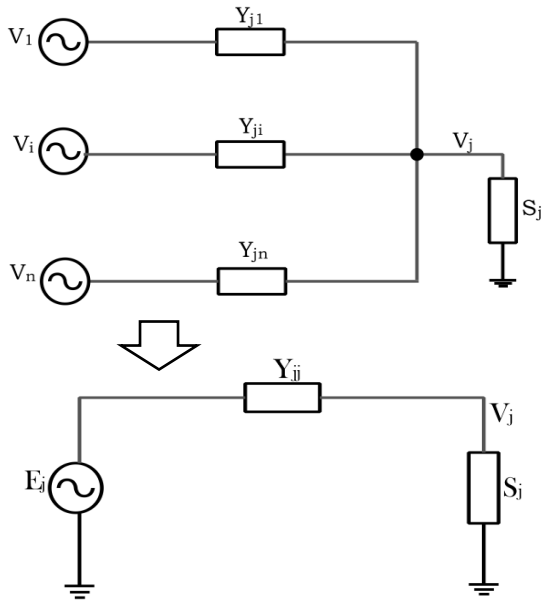The foreground representation of the network and load as viewed from the load bus is shown in Figure 1.

Figure 1. Representation of reduced local network viewed from load bus j

If we look at Figure 1 after the network transformation, the power flow equation at load bus j in the local network can be written as follows:

$$V_j^* [Y_j][V] = S_j^* \qquad (8)$$

where

S_j is the apparent load power

V_j is the voltage magnitude at the load bus

The network E_j equivalent voltage obtained can be determines by:

$$E_j = \frac{\sum_{k=1,k\neq j}^{n} Y_{jk} V_k}{Y_{jj}} \qquad (9)$$

Substituting Eq. (8) into Eq. (9) will give the load flow equation of the reduced network:

$$V_j^* (E_j - V_j) Y_{jj} = S_j^* \qquad (10)$$

The phenomenon of line voltage collapse has an association with operation at a limit where the maximum power is to be transmitted. A simplified theory of voltage stability of a two-bus system can be derived from the optimal impedance solution. We assume that a load impedance $Z\angle\emptyset$ is fed source V_S as constant voltage, with internal impedance $Z\angle\beta$ as in Figure 2.
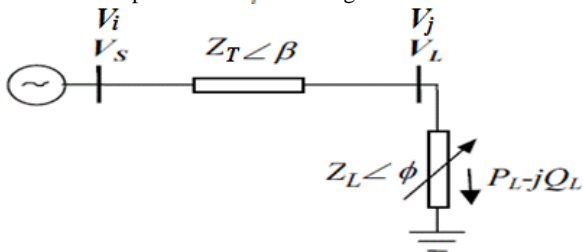

Figure 2. Simple two bus system

The assumption to be made is that constant power factor for the modelled load as where the magnitude of the load impedance may be varied- Z varies while its angle $\angle\emptyset$ constant. Voltage at the terminal of the load decreases in proportion to the current. As the load increases, current I that circulates in the system increases leading to the voltage drop. The absorbed maximum power from

the source depends on equivalent impedance between load and source. The active power transmitted to the load is expressed below (41):

$$I = \frac{V_S}{\sqrt{(Z_T\cos\beta + Z_L\cos\emptyset)^2 + (Z_T\sin\beta + Z_L\sin\emptyset)^2}} \qquad (11)$$

The short circuit current I_{CC} at the terminal of the load equals:

$$I_{CC} = \frac{V_S}{Z_T} \qquad (12)$$

Through several mathematical manipulations, the current I expression can be rewritten as follows:

$$I = \frac{I_{CC}}{\sqrt{1 + \left(\frac{Z_L}{Z_T}\right)^2 + \frac{2Z_L}{Z_T}\cos(\beta - \emptyset)}} \qquad (13)$$

Accordingly the load voltage V_L can be calculated as:

$$V_L = Z_L I$$
$$= \frac{Z_L I_{CC}}{\sqrt{1 + \left(\frac{Z_L}{Z_T}\right)^2 + \frac{2Z_L}{Z_T}\cos(\beta - \emptyset)}} \qquad (14)$$

Thus the active power at load P_L is:

$$P_L = V_L I \cos\emptyset$$
$$= \frac{Z_L I_{CC}^2}{\left[1 + \left(\frac{Z_L}{Z_T}\right)^2 + \frac{2Z_L}{Z_T}\cos(\beta - \emptyset)\right]}\cos\emptyset$$
$$= \frac{(V_S)^2/Z_S}{\left[1 + \left(\frac{Z_L}{Z_T}\right)^2 + \frac{2Z_L}{Z_T}\cos(\beta - \emptyset)\right]}\cdot\frac{Z_L}{Z_T}\cos\emptyset \qquad (15)$$

The plots of current, voltage and active power curves as a function of load demand variation for case tan β =10and tan ϕ =0.1, shown in Figure 3.In this plot, the parameter values are normalized to enable the results to be applicable to any value of load demand Z_L.
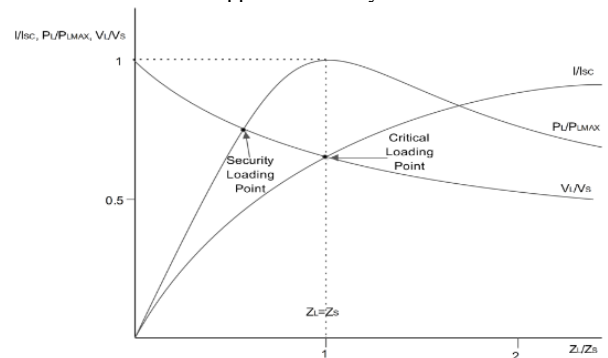

Figure 3. Electrical characteristics of a two bus system.

Figure 3 shows, the load active power P_L calculated from (15) increases when $Z_L > Z_T$. The maximum power transferred to the load is obtained when $\partial P_L/\partial Z_L = 0$ which also corresponds to $Z_L/Z_T = 1$. Beyond this maximum point, the voltage at load terminal V_L decreases below the satisfactory operational limit. The corre-

sponding point is known as the critical loading point of the local load bus.

In DC circuits theorem, the states of MPT is that load resistance is equal to the internal source resistance to reach the maximum power is transferred. Analogous to AC circuit condition, the maximum power transfer condition can be achieved when the load impedance Z_L is a conjugate of source impedance or the venin impedance Z_{Th} (42, 43) as shown in Figure 2. The magnitudes of the source and load are equal for both resistance and reactance although the reactance carries an opposite sign. The focus of this work rests in the application of the MPT theorem on AC circuit. Both resistance and reactance are taken into account in the impedance calculation. The source impedance Z_S can be written as:

$$Z_T = R_T + jX_T \tag{16}$$

The interest is to look for the value of load resistance R_L and load reactance X_L such that the amount of active power that can be delivered to the load. The active transfer power P_t at the load can be written as follows:

$$P_t = \frac{V_i V_j \sin\delta}{X_{ij}} \tag{17}$$

Form Figure 1, the interest in power flow calculation is to know the maximum transferable active power P_{max} from the source to the load. As established from the theorem, the maximum load active power is achieved when the load impedance is equal to the complex conjugate of source impedance i.e. $R_L = R_S$ and $X_L = -X_T$. Therefore, the maximum real power absorbed by the load P_{Tmax} can be expressed as:

$$P_{Tmax} = Y_{ij}(V_i * V_j) \tag{18}$$

The formulation of the proposed voltage stability index called maximum power stability index (MLSI) starts with the transformation of a multiple-node network into a two-node equivalent as shown in Figure 1. In reference to the theory of voltage stability, Chebbo (44) pointed out that there is a maximum limit of power transferable by the network. The condition speaks for a critical loading point that must be avoided to preserve the stability. At critical loading point the amount of load active power PL and maximum load active power PLmax has come to the same level. As such, this critical condition is used to define the collapse criterion of the stability index established as

$$\frac{P_T}{P_{Tmax}} \leq 1 \tag{19}$$

Insert Eq.(9) into P_{Lmax} from Eq.(18) and replacing it and P_T from Eq.(17) and into (19) resulting in the final expression of the proposed index:

$$MLSI = \frac{V_i \sin\delta}{X_{ii} * \sum_{k=1, k\neq j}^{n} Y_{kj} V_k} \tag{20}$$

The MLSI index value offers some information on the power system voltage stability. As voltage instability normally begins from local areas, different load buses may have a variety of index values. A weak bus with a high index value is deemed the most susceptible to voltage collapse. Consistent with other VSI indices, two distinct conditions carried by the index suggest that the evaluated load bus:
1. Is unstable when MPSI value is close to 1.

2. Is stable when MPSI value is close to 0.

5. Results And Discussion

The IEEE 30-bus test systems have been used for evaluating the performance and accuracy of all voltage stability indices. The IEEE 30-bus system as shown in Figure 4, consist of 6 generator bus, 24 loads bus and 41 transmission lines (45). For simulations, the indices are used to study the test systems stability for different disturbances, load increase and line disconnections. Line contingencies of the systems are studied to show that the indices are useful for line contingency ranking. Some additional aspects of firefly algorithm to optimize for load shading and DG rescheduling are identified. Transmission line overloading analysis was adopted to identify the most critical line have been selected distrusted system. All the results are produced with the help of a program developed in the Matlab software.
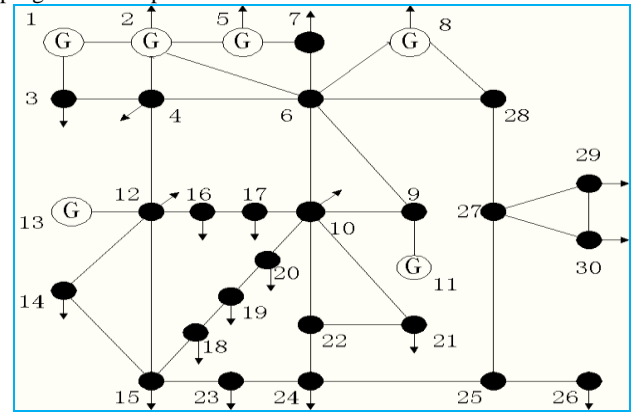

Figure 4. IEEE 30-bus system

Generally, all the implemented tests have 25 levels or stages of load increase and each stage of increment represents 0.1 multiplied by the base case load of the selected load bus. The increment begins from the base case load of a certain load bus and then gradually increases until reach to the maximum loadability of that load bus. For the IEEE 30-bus system, bus number 24 was chosen as an example to show the effect of the load change contingency on that bus.

5.1 Load change contingency

In this test, load change contingency was implemented on the load buses of the IEEE 30-bus System. The loadability of the system was investigated when considering the three different loading cases. For static approach, the voltage stability indices are good indicators for ranking the critical lines and buses. All indices are calculated under the increase of load is continued until the load flow is diverged. In the first case, single bus active power and reactive power changes for each load level at bus 24 and running continuation power flow to get the corresponding voltages of the buses. The load at bus 24 has increased slowly varied from its base value (P_{24} & Q_{24}) by steps at 2.5*(P_{24} & Q_{24}). Tests were conducted by gradually increasing the active power and reactive power loading at selected bus and the indices values for lines connected to that bus were increased and have highest values compared to other lines to indicate that it is the most critical one.

From Figure 5 (a,b,c and d) , it is observed that the indices values at the lines connected to bus 24 were increasing accordingly as the active and reactive power loading at bus 24 were gradually increased. It can be seen that at the maximum active and reactive power loading, the indices values for lines 31, 32 and 33 reach their maximum values. At this point, line 31 gives the highest value for all indices. Thus, this line is close to its voltage stability limit and any further increase in active and reactive power loading at bus 24 would cause the MLSI value at line 31 to exceed unity

since this line is connected directly to bus 24. This implies that MLSI is the most sensitive index among the proposed indices and line 31 has reached its unstable condition, which may lead to voltage collapse to the entire system. Bus 24 is expected to operate at the loading condition less than this point so that secure operation could be maintained. The trend of indices values at each line connected to bus 24 when active and reactive power loading at this bus was increased has been illustrated in Figure 5(e) that indices values were increased accordingly to the loading increment. It is also observed that line 31 has the highest value for all indices and then can be considered as the most sensitive line.

In Figure 5, the indices values on line 31 were tabulated to compare all indices for the same line. It is clear that MLSI has the highest value among other indices. Also, it is observed that FVSI value was the highest one after MLSI, and then LQP was coming in the sequence.
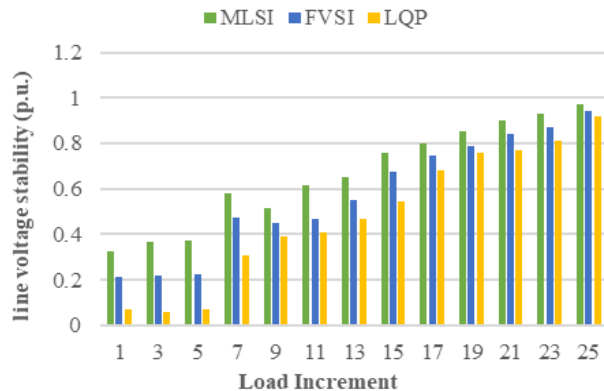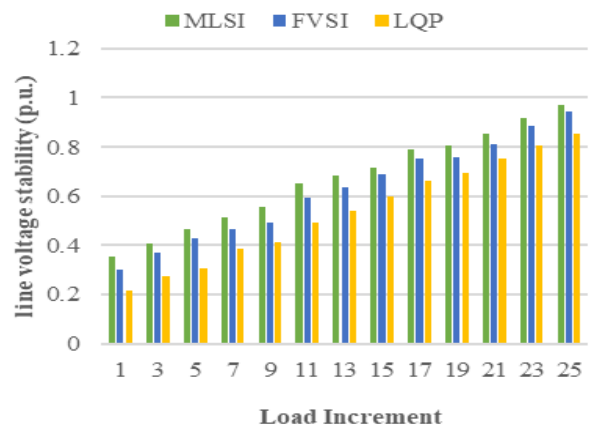

Figure 5. Effect of increasing (P_{24} & Q_{24}) at Bus 24 to MLSI, FVSI and LQP evaluated for Line 31.

In the second case, single bus active power change for each load level at bus 24 and running continuation power flow to get the corresponding voltages of the buses. The load at bus 24 has increased slowly varied from its base value (P_{24}) by steps at $2.5*(P_{24})$. Tests were conducted by gradually increasing the active power loading at selected bus and the indices values for lines connected to this bus were increased and have highest values compared to others lines to indicate that it is the most critical one.

From the Figure 6 (a,b,c and d), it is observed that the indices values at the lines connected to bus 24 were increasing accordingly as the active power loading at bus 24 were gradually increased. It can be seen that at the maximum active power loading, the indices values for lines 31, 32 and 33 reach their maximum values. At this point, line 31 gives the highest value for all indices. Thus, this line is close to its voltage stability limit and any further increase in active power loading at bus 24 would cause the MLSI value at line 31 to exceed unity since this line is connected directly to bus 24. This implies that MLSI is the most sensitive index among the proposed indices and line 31 has reached its unstable condition, which may lead to voltage collapse to the entire system. Bus 24 is expected to operate at the loading condition less than this point so that secure operation could be maintained. The trend of indices values at each line connected to bus 24 when active power loading at this bus was increased has been illustrated in Figure 6(e) that indices values are increased accordingly to the loading increment. It is also observed that line 31 has the highest value for all indices and then can be considered as the most sensitive line.

In Figure 6, the indices values on line 31 are tabulated to compare all indices at the same line. From that table it is clear that MLSI has the highest value among other indices. Also, it is observed that LQP has a highest after MLSI, and then FVSI was coming in the sequence.

Figure 6. Effect of increasing (P_{24}) at Bus 24 to MLSI, FVSI and LQP evaluated for Line 31.

In the third case, single bus reactive power change for each load level at bus 24 and running continuation power flow to get the corresponding voltages of the buses. The load at bus 24 is increased slowly varied from its base value (Q_{24}) by steps at $2.5*(Q_{24})$. Tests were conducted by gradually increasing the reactive power loading at selected bus and the indices values for lines connected to this bus were increased and have highest values compared to others lines to indicate that it is the most critical one.

From the Figure 7 (a,b,c and d), it is observed that the indices values at the lines connected to bus 24 were increasing accordingly as the reactive power loading at bus 24 were gradually increased. It can be seen that at the maximum reactive power loading, the indices values for lines 31, 32 and 33 reach their maximum values. At this point, line 31 gives the highest value for all indices. Thus, this line is close to its voltage stability limit and any further increase in reactive power loading at bus 24 would cause the MLSI value at line 31 to exceed unity. This implies that MLSI is the most sensitive index among the proposed indices and line 31 has reached its unstable condition, which may lead to voltage collapse to the entire system. Bus 24 is expected to operate at the loading condition less than this point so that secure operation could be maintained. The trend of indices values at each line connected to bus 24 when reactive power loading at that bus was increased has been illustrated in Figure 7(e) that indices values were increased accordingly with respect to the loading increment. It is also observed that line 31 has the highest value for all indices and then can be considered as the most sensitive line.

In Figure 7, the indices values on line 31 were tabulated to compare all indices at the same line. From that table it is clear that MLSI has the highest value among other indices. Also, it is observed that FVSI has a highest after MLSI, and then LQP was coming in the sequence.
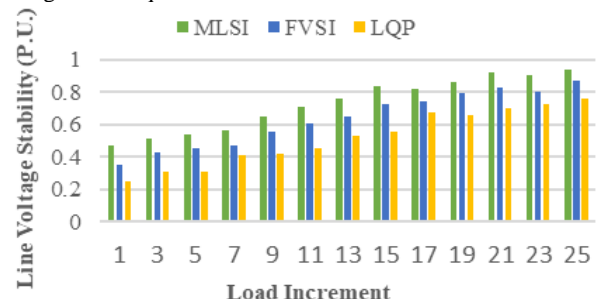
Figure 7. Effect of increasing (Q_{24}) at Bus 24 to MLSI, FVSI and LQP evaluated for Line 31.

5.2 Line Contingency

Line contingency was implemented on two lines connected to the bus 24 in the IEEE 30-bus System. These two lines are line 31, which connecting between bus 24 and bus 22, and line 32, which connecting between bus 24 and bus23. The loadability of the sys-

tem was investigated when considering the loading cases. In the first case, line contingency was implemented on line 31, which means disconnecting line 31, and then single bus active power and reactive power changes for each load level at bus 24 and running continuation power flow to get the corresponding voltages of the buses. The load at bus 24 has increased slowly varied from its base value (P_{24} & Q_{24}) to the level of voltage collapse at $2.5*(P_{24}$ & Q_{24}). Tests were conducted by gradually increasing the active power and reactive power loading at selected bus and the indices values for the remaining lines connected to that bus which increased and had highest values when compared to others lines. That indicates the remaining lines showed the most critical situation.

From the Figure 8 (a,b,c and d), it is observed that the indices values at the remaining lines connected to bus 24 which increased accordingly as the active power and reactive power loading were gradually increased. It can be noticed, at the maximum active power and reactive power loading, the indices values for lines 32 and line 33 reached their maximum values. At this point, line 32 gives the highest value for all indices. Thus, this line is close to its voltage stability limit and any further increase in power loading at bus 24 would cause the MLSI value at line 32 to exceed unity. This implies that MLSI is the most sensitive index among the proposed indices and line 32 has reached its unstable condition, which may lead to voltage collapse to the entire system. The trend of indices values at lines 32 and line 33 connected to bus 24 was illustrated in Figure 8(e) that indices values were increased accordingly to the loading increment. It is also observed that line32 has the highest value for all indices and then it can be considered as the most sensitive line.

In Figure 8, the indices values of line 32 were tabulated to compare all indices at the same line. From that table it is clear that MLSI has the highest value among other indices. Also, it is observed that FVSI value was the highest one after MLSI, and then LQP was coming in the sequence.
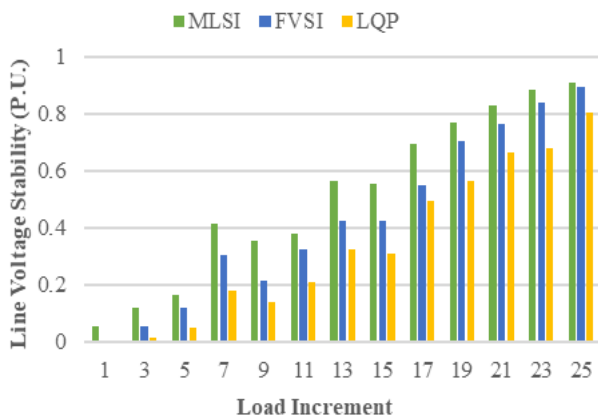

Figure 8. Line Contingency Effect of Line 31 to MLSI, FVSI and LQP evaluated for Line 32.

In the second case, line contingency was implemented on line 32, which means disconnecting line 32, then single bus active power and reactive power change for each load level at bus 24 and running continuation power flow to get the corresponding voltages of the buses. The load at bus 24 was increased slowly varied from its base value (P_{24} & Q_{24}) by steps at $2.5*(P_{24}$ & Q_{24}). Tests were conducted by gradually increasing the active power and reactive power loading at selected bus and the indices values for the remaining lines connected to that bus were increased and have highest values compared to others lines to indicate that it is the most critical one.

From Figure 9 (a,b,c and d), it is observed that the indices values at the remaining lines connected to bus 24 were increasing accordingly as the active power and reactive power loading at bus 24 were gradually increased. It can be seen that at the maximum active power and reactive power loading, the indices values for lines31 and line33 reach their maximum values. At this point, line

31 gives the highest value for all indices. Thus, this line is close to its voltage stability limit and any further increase in power loading at bus 24 would cause the MLSI value at line 31 to exceed unity. This implies that MLSI is the most sensitive index among the proposed indices and line 31 has reached its unstable condition, which may lead to voltage collapse to the entire system. The trend of indices values at lines 31 and line 33 connected to bus 24 when active power and reactive power loading at that bus were increased is illustrated in Figure 9(e) that indices values were increased accordingly to the loading increment. It is also observed that line 31 has the highest value for all indices and then can be indicated as the most sensitive line.
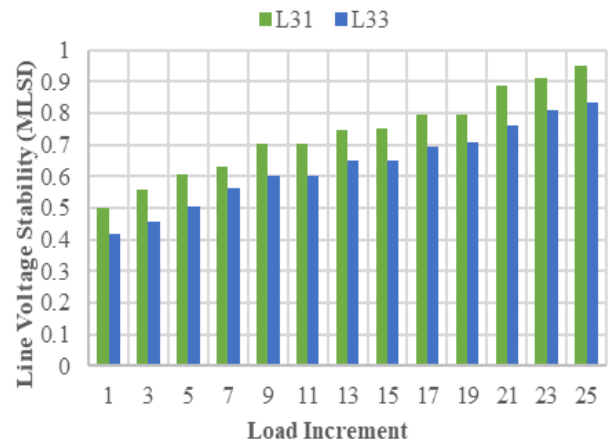

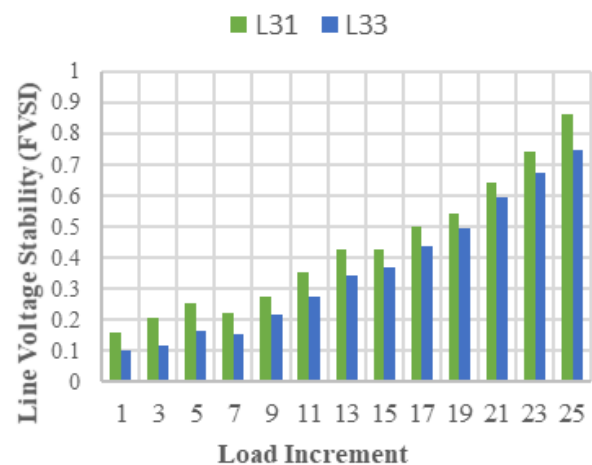**Figure 9(a)**. Line Contingency Effect of Line 32 to MLSI evaluated for Lines 31 and 33.

Figure 9(b). Line Contingency Effect of Line 32 to FVSI evaluated for Lines 31 and 33.
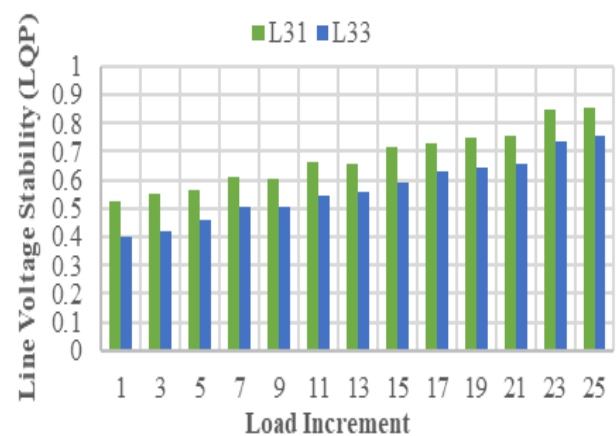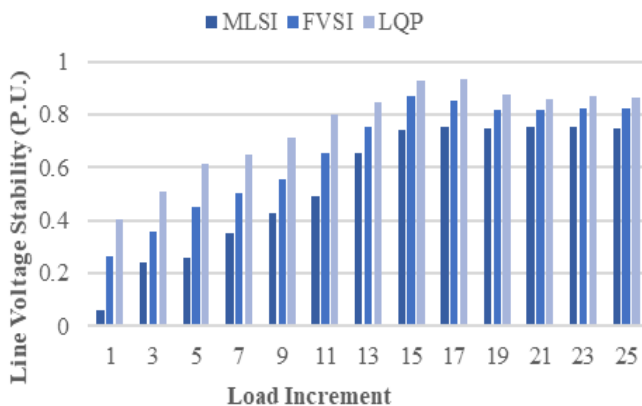

Figure 9(c). Line Contingency Effect of Line 32 to LQP evaluated for Lines 31 and 33.

In Figure 9, the indices values on line 31 were tabulated to compare all indices at the same line. From that table it is clear that MLSI has the highest value among other indices. Also, it is observed that LQP has a highest after MLSI, and then LVSI and FVSI were coming in the sequence, respectively. All these indices values for line 31 are illustrated in Figure 4.12.

Figure 9. Line Contingency Effect of Line 32 to MLSI, FVSI and LQP evaluated for Line 31.

6. Conclusion

In this study, the improved line voltage stability is introduced as proposed MLSI index. Maximum line stability index is a fast and reliable tool to analyze the state of voltage stability in power system. The index is used to identify critical line that determine the maximum power transfer in the system. The critical lines which represent optimum DG level are identified. The impact of load level is evaluated based on the function which minimizes the total active power loss. The simulation results indicated that the overall impact of the DG units on line voltage stability is achieved.

References

[1] Jauch C, Matevosyan J, Ackermann T, Bolik S. International comparison of requirements for connection of wind turbines to power systems. Wind energy. 2005;8(3):295-306.
[2] Eriksen PB, Ackermann T, Abildgaard H, Smith P, Winter W, Garcia JR. System operation with high wind penetration. IEEE Power and Energy Magazine. 2005;3(6):65-74.
[3] Piwko R, Osborn D, Gramlich R, Jordan G, Hawkins D, Porter K. Wind energy delivery issues [transmission planning and competitive electricity market operation]. IEEE Power and Energy Magazine. 2005;3(6):47-56.
[4] Karbalaei F, Soleymani H, Afsharnia S, editors. A comparison of voltage collapse proximity indicators. IPEC, 2010 Conference Proceedings; 2010: IEEE.
[5] Conroy J, Watson R. Low-voltage ride-through of a full converter wind turbine with permanent magnet generator. IET Renewable Power Generation. 2007;1(3):182-9.
[6] Mullane A, Lightbody G, Yacamini R. Wind-turbine fault ride-through enhancement. IEEE Transactions on Power Systems. 2005;20(4):1929-37.
[7] Ummels BC, Gibescu M, Pelgrum E, Kling WL, Brand AJ. Impacts of wind power on thermal generation unit commitment and dispatch. IEEE Transactions on energy conversion. 2007;22(1):44-51.
[8] Causebrook A, Atkinson DJ, Jack AG. Fault ride-through of large wind farms using series dynamic braking resistors (March 2007). IEEE Transactions on power systems. 2007;22(3):966-75.
[9] Molinas M, Suul JA, Undeland T. Low voltage ride through of wind farms with cage generators: STATCOM versus SVC. IEEE Transactions on power electronics. 2008;23(3):1104-17.
[10] Acharya N. Security, protection, and control of power systems with large-scale wind power penetration: Iowa State University; 2010.
[11] Vaziri M, Vadhva S, Oneal T, Johnson M, editors. Smart grid, distributed generation, and standards. Power and Energy Society General Meeting, 2011 IEEE; 2011: IEEE.

[12] Energy G. The effects of integrating wind power on transmission system planning, reliability, and operations. Report on phase. 2005;2.
[13] Di Florio G. Innovative model of product certification within the energy deregulated market. example of application to a smart energy area in the sector of local transport service. 2015.
[14] Hussain S, Kim Y-C, editors. Fault resilient communication network architecture for monitoring and control of wind power farms. Advanced Communication Technology (ICACT), 2016 18th International Conference on; 2016: IEEE.
[15] Akorede MF, Hizam H, Pouresmaeil E. Distributed energy resources and benefits to the environment. Renewable and Sustainable Energy Reviews. 2010;14(2):724-34.
[16] Viral R, Khatod D. Optimal planning of distributed generation systems in distribution system: A review. Renewable and Sustainable Energy Reviews. 2012;16(7):5146-65.
[17] Hemdan N, Kurrat M, editors. Influence of distributed generation on different loadability aspects of electric distribution systems. CIRED, IET Conference; 2009: IET.
[18] Boroyevich D, Cvetkovic I, Burgos R, Dong D. Intergrid: A future electronic energy network? IEEE Journal of Emerging and Selected Topics in Power Electronics. 2013;1(3):127-38.
[19] Olivares DE, Mehrizi-Sani A, Etemadi AH, Cañizares CA, Iravani R, Kazerani M, et al. Trends in microgrid control. IEEE Transactions on smart grid. 2014;5(4):1905-19.
[20] Hasani M, Parniani M, editors. Method of combined static and dynamic analysis of voltage collapse in voltage stability assessment. Transmission and Distribution Conference and Exhibition: Asia and Pacific, 2005 IEEE/PES; 2005: IEEE.
[21] Manwell JF, McGowan JG, Rogers AL. Wind energy explained: theory, design and application: John Wiley & Sons; 2010.
[22] Azmy AM, Erlich I, editors. Impact of distributed generation on the stability of electrical power system. Power Engineering Society General Meeting, 2005 IEEE; 2005: IEEE.
[23] El-Khattam W, Salama M, editors. Impact of distributed generation on voltage profile in deregulated distribution system. Proceedings of the Power Systems 2002 Conference, Impact of Distributed Generation, Clemson, SC, USA; 2002.
[24] Morison G, Gao B, Kundur P. Voltage stability analysis using static and dynamic approaches. IEEE transactions on Power Systems. 1993;8(3):1159-71.
[25] Lamsal D, Mishra A, Gautam P, editors. Optimal location and sizing of distributed generation: B-coefficient matrix approach. Control and Automation (ICCA), 2016 12th IEEE International Conference on; 2016: IEEE.
[26] Ettehadi M, Ghasemi H, Vaez-Zadeh S. Voltage stability-based DG placement in distribution networks. ieee transactions on power delivery. 2013;28(1):171-8.
[27] Al Abri R, El-Saadany EF, Atwa YM. Optimal placement and sizing method to improve the voltage stability margin in a distribution system using distributed generation. IEEE transactions on power systems. 2013;28(1):326-34.
[28] Weron R. Modeling and forecasting electricity loads and prices: A statistical approach: John Wiley & Sons; 2007.
[29] Cherry DD. Optimal placement of distributed generation on a power system using particle swarm optimization: Mississippi State University; 2012.
[30] Taylor SA, Baker TL. An assessment of the relationship between service quality and customer satisfaction in the formation of consumers' purchase intentions. Journal of retailing. 1994;70(2):163-78.
[31] Kundur P, Balu NJ, Lauby MG. Power system stability and control: McGraw-hill New York; 1994.
[32] Kundur P, Paserba J, Ajjarapu V, Andersson G, Bose A, Canizares C, et al. Definition and classification of power system stability IEEE/CIGRE joint task force on stability terms and definitions. IEEE transactions on Power Systems. 2004;19(3):1387-401.
[33] Lopes JP, Hatziargyriou N, Mutale J, Djapic P, Jenkins N. Integrating distributed generation into electric power systems: A review of drivers, challenges and opportunities. Electric power systems research. 2007;77(9):1189-203.
[34] Lof P-A, Andersson G, Hill D. Voltage stability indices for stressed power systems. IEEE transactions on power systems. 1993;8(1):326-35.
[35] Moghavvemi M, Faruque M. Power system security and voltage collapse: a line outage based indicator for prediction. International Journal of Electrical Power & Energy Systems. 1999;21(6):455-61.
[36] 36. Vaahedi E, Fuchs C, Xu W, Mansour Y, Hamadanizadeh H, Morison G. Voltage stability contingency screening and ranking. IEEE Transactions on power systems. 1999;14(1):256-65.

[37] 37. Kumar YP, Raju HP. Static voltage stability margin enhancement using shunt compensating devices. 2013.

[38] Musirin I, Rahman TA, editors. Novel fast voltage stability index (FVSI) for voltage stability analysis in power transmission system. Research and Development, 2002 SCOReD 2002 Student Conference on; 2002: IEEE.

[39] Verbic G, Gubina F, editors. A novel concept for voltage collapse protection based on local phasors. Transmission and Distribution Conference and Exhibition 2002: Asia Pacific IEEE/PES; 2002: IEEE.

[40] Moghavvemi M, Omar F. Technique for contingency monitoring and voltage collapse prediction. IEE Proceedings-Generation, Transmission and Distribution. 1998;145(6):634-40.

[41] Chebbo A, Irving M, Sterling M, editors. Reactive power dispatch incorporating voltage stability. IEE Proceedings C (Generation, Transmission and Distribution); 1992: IET.

[42] Schauder C, Gernhardt M, Stacey E, Lemak T, Gyugyi L, Cease T, et al. Development of a/spl plusmn/100 MVAr static condenser for voltage control of transmission systems. IEEE Transactions on Power Delivery. 1995;10(3):1486-96.

[43] Glisson Jr TH. Complex Power. Introduction to Circuit Analysis and Design: Springer; 2011. p. 479-520.

[44] Chebbo A, Irving M, Sterling M, editors. Voltage collapse proximity indicator: behaviour and implications. IEE Proceedings C (Generation, Transmission and Distribution); 1992: IET.

[45] Wang C, Nehrir MH. Analytical approaches for optimal placement of distributed generation sources in power systems. IEEE Transactions on Power systems. 2004;19(4):2068-76.